32, 5901. (b) Bianchini, C.; Barbaro, P.; Meli, A.; Peruzzini, M.; Vacca, A.; Vizza, F. *Organometallics* **1993**, *12*, 2505. (c) Rahim, M.; Bushweller, C. H.; Ahmed, K. J. *Organometallics* **1994**, *13*, 4952.
6. Werner, H.; Baum, M.; Schneider, D.; Windmüller, B. *Organometallics* **1994**, *13*, 1089.
7. Werner, H.; Gevert, O.; Steinert, P.; Wolf, J. *Organometallics* **1995**, *14*, 1786.
8. Kang, S. K.; Song, J. S.; Moon, J. H.; Yun, S. S. submitted for publication.
9. Frisch, M. J.; Trucks, G. W.; Schlegel, H. B.; Gill, P. M. W.; Johnson, B. G.; Robb, M. A.; Cheeseman, J. R.; Keith, T. A.; Petersson, G. A.; Montgomery, J. A.; Raghavachari, K.; Al-Laham, M. A.; Zakrzewski, V. G.; Ortiz, J. B.; Foresman, J.; Cioslowski, B.; Stefanov, B.; Nanayakkara, A.; Challacombe, M.; Peng, C. Y.; Ayala, W.; Chen, W.; Wong, M. W.; Andres, J. L.; Replogle, E. S.; Gomperts, R.; Martin, R. L.; Fox, D. J.; Binkley, J. S.; Defrees, D. J.; Baker, J.; Stewart, J. P.; Head-Gordon, M.; Gonzalez, C.; Pople, J. A. Gaussian, Inc., Pittsburgh PA, 1995.
10. Hay, P. J.; Wadt, W. R. *J. Chem. Phys.* **1985**, *82*, 270.
11. Wadt, W. R.; Hay, P. J. *J. Chem. Phys.* **1985**, *82*, 284.
12. Binkley, J. S.; Pople, J. A.; Hehre, W. J. *J. Am. Chem. Soc.* **1980**, *102*, 939.
13. Hehre, W. J.; Stewart, R. F.; Pople, J. A. *J. Chem. Phys.* **1969**, *51*, 2657.
14. Hay, P. J.; Wadt, W. R. *J. Chem. Phys.* **1985**, *82*, 299.
15. Hariharan, P. C.; Pople, J. A. *Theor. Chim. Acta* **1973**, *28*, 213.
16. (a) Busetto, C.; D'Alfonso, A.; Maspero, F.; Perego, G.; Zazetta, A. *J. Chem. Soc., Dalton Trans.* **1977**, 1828. (b) Hietkamp, S.; Stufkens, D. J.; Vrieze, K. *J. Organomet. Chem.* **1977**, *139*, 189. (c) Werner, H.; Wolf, J.; Höhn, A. *J. Organomet. Chem.* **1985**, *287*, 395. (d) Höhn, A.; Otto, H.; Dziallas, M.; Werner, H. *J. Chem. Soc., Chem. Commun.* **1987**, 852.
17. (a) Stockis, A.; Hoffmann, R. *J. Am. Chem. Soc.* **1980**, *102*, 2952. (b) Kang, S. K.; Albright, T. A.; Silvestre, *J. Croat. Chim. Acta,* **1984**, 1355. (c) Albright, T. A.; Burdett, J. K.; Whangbo, M.-H. *Orbital Interactions in Chemistry*; Wiley; New York, 1985.
18. The C-C distance in a free HC≡CH is optimized to be 1.188 Å and 1.186 Å at 3-21G (referred to as ECP1) and 6-31G* (ECP2) basis sets. The experimental value is 1.20 Å.
19. (a) Koga, N.; Morokuma, K. *J. Am. Chem. Soc.* **1993**, *115*, 6883. (b) Lin, Z.; Hall, M. B. *J. Am. Chem. Soc.* **1994**, *116*, 4446. (c) Yoshida, T.; Koga, N.; Morokuma, K. *Organometallics* **1995**, *14*, 746. (d) Ehlers, A. W.; Dapprich, S.; Vyboishchikov, S. F.; Frenking, F. *Organometallics* **1996**, *15*, 105.
20. Baum, M.; Mahr, N.; Werner, H. *Chem. Ber.* **1994**, *127*, 1877.
21. Wolf, J.; Werner, H.; Serhadli, O.; Ziegler, M. L. *Angew. Chem.* **1983**, *95*, 428; *Angew. Chem. Int. Ed. Engl.* **1983**, *22*, 414.

Analytical Characteristics and Applications of Laser Ionization Mass Spectrometry

Hoong-Sun Im*, Ha-Sub Yoon†, and Seong Kyu Kim†

Surface Analysis Group, Korea Research Institute of Standards and Science, Taejon 305-600, Korea
†Department of Chemistry, Sung Kyun Kwan University, Suwon 440-746, Korea
Received August 23, 1996

We have built a laser ionization mass spectrometer (LIMS) for chemical composition analysis of solid samples, which employs an Nd:YAG laser and a time-of-flight mass analyzer. In this spectrometer, the maximum mass we identified clearly is higher than 2000 amu. A mass resolution of 230 has been achieved at m/z 208 (Pb element) in the linear TOFMS and can be even improved up to 1550 by employing a reflectron. The detection limit is determined to be on the order of ppm for Fe and In. The depth resolution is found to be about 20 Å/spectrum with a laser power of 0.5 J/cm^2. We also report a preliminary application of the LIMS to identifying impurities resident in several solid samples.

Introduction

Recently, the development of chemical composition analysis technique for solid samples has rapidly grown. The techniques have adapted sputtering method to take off compositional elements or molecules from the surface of a sample. Among them, laser ionization mass spectroscopy (LIMS)[1] is one of the promising analytical techniques. In this technique, the composition of a solid sample can be identified by measuring the mass of elemental or molecular ions produced by the interaction between a focused high-power laser pulse and a target surface. This technique has

*Author to whom correspondence should be addressed.

been applied to grasp the chemical composition of many solid materials such as electronic devices,[2] ores,[3] insulators,[4] and biological materials.[5] These materials are not amenable to analysis by conventional mass spectrometries because they are thermally labile or nonvolatile.

LIMS has several unique characteristics compared with other conventional mass spectrometries due to the direct evaporation and ionization of elements from the target. It has shown the capability of the compositional analysis for conducting or non-conducting solid samples in bulk or in thin film. Also the sample preparation for analysis is so simple that rapid analysis is possible. These capabilities are superior to the conventional methods. LIMS can also analyze elemental composition in the micro-area of samples since ions are extracted out of focused spot of the laser beam.

Although various mass analyzers have been used in LIMS, the time-of-flight mass analyzer has generally been the most suitable as the ion source is a pulsed type and fast digitizing electronics for time-of-flight measurement are available.[6] TOFMS has a number of advantages such as high ion transmission, a theoretically unlimited mass range, and the ability to obtain a complete mass spectrum in a few microseconds.[7] The main limitation of TOFMS, however, is the low mass resolution. Two factors limiting the mass resolution are the space spread and the energy spread of the ions created initially in the ionization region of the TOF device. In LIMS, the energy spread is more serious problem than the other one. The effect of the energy spread cannot be removed completely in TOFMS, but can be only reduced by compensating the energy difference using a reflectron in TOFMS. The reflectron is an electrostatic ion mirror, which was originally invented by Mamyrin in 1966.[8] In the reflectron TOFMS, the ions with higher energy travel a longer path than those with lower energy. Thus, with the proper parameters of the reflectron system, the ions with a wide range of energies can arrive at the detector simultaneously. This improves the mass resolution of TOFMS.

In this present work, we report the analytical characteristics-the mass range, the mass resolution, the sensitivity, and the depth resolution-of the home-built LIMS and its application to the identification of impurities in solid samples.

Experimental Method

The schematic drawing of the LIMS developed in our laboratory is shown in Figure 1. The system consists of the ionization chamber and the ion drift chamber, both of which are pumped by two oil diffusion pumps (Korea Vacuum Corp.) to keep the working pressure in the order of 10^{-6} torr. In the ionization chamber, electrodes of ion optics-ion repelling electrode (A), extracting electrode (B), ground electrodes (C), and ion deflecting electrodes (E) (upward and rightward tuning electrodes) are placed as shown in Figure 1. The repelling electrode has a hole of 10 mm diameter at the center. In the extracting electrode, there is a hole of 1 mm diameter to select the center part of the produced ions. The skimmed ions are directed to the active area of a microchannel plate (MCP) detector (Galileo Electro-Optics Corp.; Model TOF-2003) which is attached at the end of the ion drift chamber using the ion deflecting electrodes. The overall flight path length is about 139 cm including the extracting distance of 4 cm. During the experiments, the DC voltage of 2500 V has been supplied to the ion repelling electrode and 140 V to the upward deflecting electrodes. Other electrodes have been set to the ground voltage.

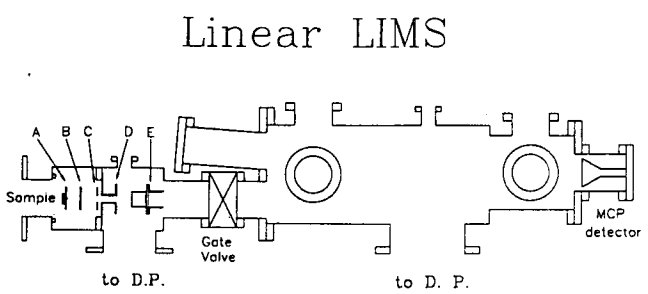

Figure 1. Schematic drawing of the home-built linear LIMS. It consists of the ionization chamber and the ion drift chamber, which are connected by a gate valve. In the ionization chamber, ion optics are installed; A-repelling electrode, B-extracting electrode, C-ground electrode, D-optics holder, E-ion deflecting electrodes.

To vaporize and ionize the sample, we used an Nd:YAG laser (Quanta-Ray; Model DCR-3) that produces pulses of 10 ns duration at the repetition rate of 10 Hz and the wavelength of 532 nm. The laser beam was delivered to samples by using several right-angle prisms. The intensity of laser beam was reduced by a pinhole of 1 mm diameter in order to get the appropriate intensity. The laser beam was focused with a glass lens of a 500 mm focal length in front of the vacuum chamber window and irradiated to sample with an angle of 45° between the laser beam and the sample surface. This gives the beam spot of approximately 300 μm diameter on the sample resulting in a power density of 0.5-0.8 J/cm^2.

A sample was held by a teflon sample holder and covered with a stainless steel cap. The sample holder was mounted at the tip of a rotary-linear motion feedthrough (MDC; BRML-275) and then this motion feedthrough was attached to the vacuum flange. By adjusting the distance of the motion feedthrough, the sample cap should touch the repelling electrode firmly to give a solid electrical contact between the electrode and the sample. This generates better electric field in the ionization region.

The interaction between the high power laser beam and the solid sample can vaporize and ionize the elements of the sample. The ions are extracted and injected into the field free region by the electric field applied to the repelling electrode. The ions are then detected by MCP to generate a transient signal that represents the mass spectrum. The transient signal is recorded by a 300 MHz digital oscilloscope (LeCroy; 9310M) with a summed average mode. The mass spectra have been collected at the speed of 100 M sampling/sec (10 ns time resolution). Each spectrum was obtained after averaging over 500 laser shots. The recorded data were then transfered to a PC *via* GPIB board for further processing. The schematic drawing of this experimental setup is depicted in Figure 2.

In order to improve the mass resolution of TOFMS, we designed a reflectron and installed it at the end of the ion drift chamber as shown in Figure 1. The detailed in-

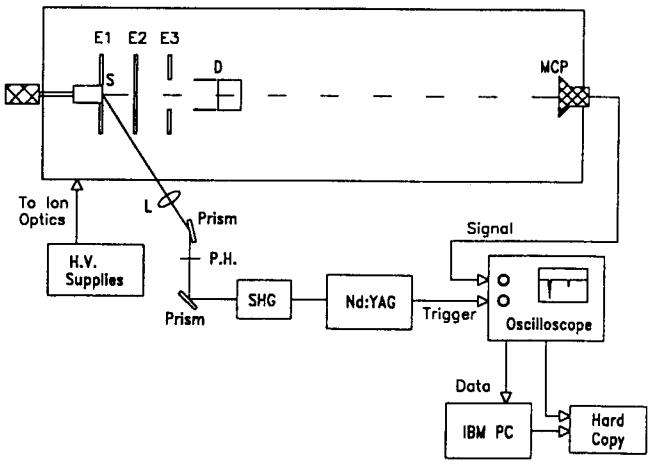

Figure 2. Schematic diagram of experimental setup (E1-repelling electrode, E2-extracting electrode, E3-ground electrode, D-ion deflecting electrodes, S-sample holder, L-lens, P.H.-pin hole). For details, see text.

formation of this reflectron will be reported elsewhere.[9] Here, only a brief description is presented. The reflectron is made of 38 stainless steel rings, which are connected with appropriate resistors to divide the applied high voltage. The total length of this reflectron is about 210 mm, which consists of decelerating part (33 mm) and reflecting part (177 mm), and is mounted on the 10" flange. All the parameters of the dimensions and applied voltages were determined from a theoretical calculation. In our experimental conditions, the decelerating voltage was set to about 1724 V and the reflecting voltage to 3400 V.

The samples used in the present work are Pb, Zn, Co thin film, Ta_2O_5 thin film, $Pb(Zr_{0.52}Ti_{0.48})O_3$ (PZT) bulk disk and PZT thin film. Pb sample of 99.999% purity was obtained from the Inorganic Analysis Group in Korea Research Institute of Standards & Science (KRISS). Zn sample was purchased from Johnson Mathey Co. The thin films of Co and Ta_2O_5 were deposited using ion beam assisted deposition (IBAD) technique and the PZT thin film was deposited by pulsed laser deposition (PLD) in our group. The PZT disk was synthesized from Ssangyong Research Center. All the samples were measured as received without any further pretreatment. A piece of a solid sample with several millimeter thickness was cut into about 10 mm in diameter, and was mounted on the teflon sample holder.

Results and Discussion

Figure 3 displays the mass spectrum for Pb sample obtained with the linear LIMS under the laser fluence of 0.8 J/cm^2. The middle part of the mass spectrum is magnified by the factor of 4 and the end part is magnified by the factor of 20 in order to show the details of the spectrum. The first main peak has been assigned as K element, which is detected in all the samples. This is due to the surface contamination from air. In LIMS experiments, Na (the first small peak in the mass spectrum) and K elements have been observed very easily if the solid sample was not cleaned thoroughly. Both elements can be used as internal ref-

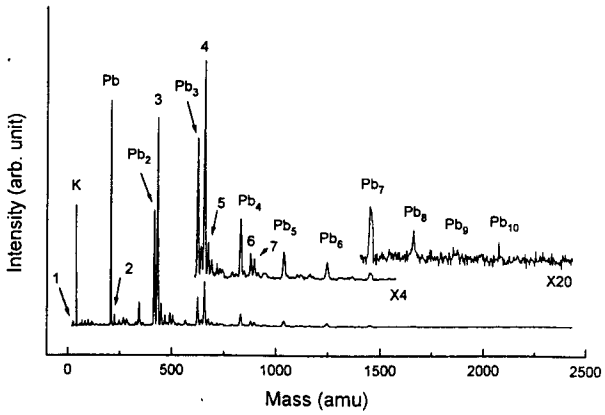

Figure 3. Mass spectrum of Pb sample obtained with the linear LIMS. The series of Pb clusters are assigned in the spectrum. The assignments of other main peaks are listed in Table 1.

Table 1. The list of the peak assignments of Pb oxides

Peak #	Mass (amu)	Assignment
1	23	Na
2	224	PbO
3	431	Pb_2O
4	654	Pb_3O_2
5	671	Pb_3O_3
6	876	Pb_4O_3
7	893	Pb_4O_4

erences for the mass calibration. With the present laser fluence, Pb clusters up to Pb_{10} as well as their oxides are clearly observed. The peaks for Pb clusters are assigned in the figure and the detailed assignments of other main peaks are listed in Table 1.

With the reduced laser fluence (0.5 J/cm^2), the mass spectra of mono-atomic Pb were obtained using the linear and the reflected LIMS, which are shown in Figure 4. The mass resolution is the ratio of a measured mass peak (m) to its width ($\triangle m$); $M_r=m/\triangle m$. Usually the full width at half maximum (FWHM) of a measured mass peak is used as the width of the peak. In TOFMS, however, an ion peak is measured as the arrival time of an element to the detector from the starting pulse, such as the laser triggering. The arrival time, t, is proportional to the mean square root of an elemental mass, m, that is, $t=am^{1/2}+b$, where a and b are experimental constants. From a simple calculation, M_r can be expressed by relating to the arrival time as $M_r=m/\triangle m=(t/2\triangle t)$,[10] where the FWHM of a time peak is usually chosen as $\triangle t$. We use this time relationship for the determination of M_r of our LIMS. In the linear LIMS, the isotopes of Pb are scarcely separated to give the mass resolution of 230. In the reflected LIMS, however, the mass resolution has increased to about 1550. These results indicate that the reflectron which was built in our laboratory helps to improve the mass resolution by the factor of almost 7.

In Figure 5, the mass spectrum of the commercial Zn sample obtained by the linear LIMS is presented. In the spectrum, the peaks of Zn and its clusters are observed as well as the surface contaminants of Na and K. In addition to these peaks, several other peaks which belong to the im-

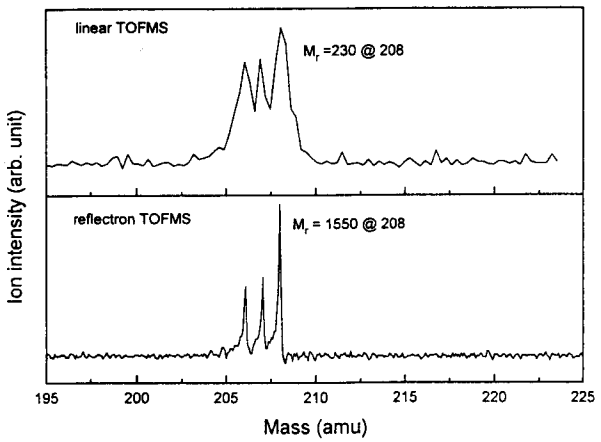

Figure 4. Mass spectra of mono-atomic Pb taken with the laser fluence of 0.5 J/cm^2 using the linear TOFMS (top) and the reflectron TOFMS (bottom). The measured mass resolutions are written in the spectra.

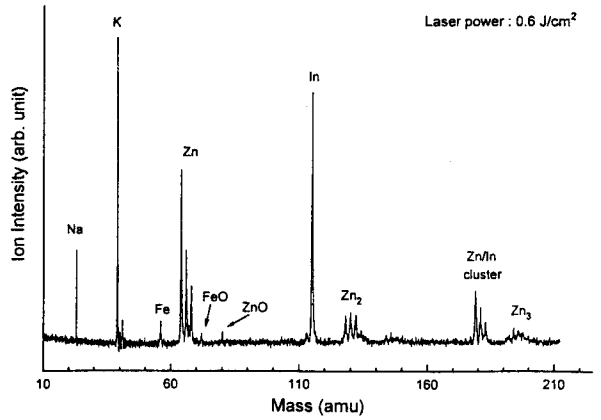

Figure 5. Mass spectrum of Zn sample obtained with the linear LIMS. The detailed assignments of the peaks are shown in the spectrum.

purities of samples appear. The detailed assignments of the peaks are reported in the figure. By comparing these results with the analysis data sheet obtained with Inductively Coupled Plasma-Optical Emission Spectroscopy (ICP-OES), as listed in Table 2, the sensitivity of this linear LIMS is determined to be on the order of ppm for In and Fe elements. Even though the data sheet indicates that there are several other impurities of Si, Ag, Cu, and Cd, we could not observe these elements in the present experiments. In addition, the peak intensity of In is larger than that of Zn in the mass spectrum. This means that the number of In ions produced by laser ablation is larger than that of Zn ions. These observations reflect the differences in the ionization probability for each element during the laser ablation process.[11] It is found that Si, Ag, and Cu require more laser fluence than Zn to obtain the ion peaks in LIMS.[12]

The information on the depth resolution of LIMS is very important for the application of LIMS to thin film samples. In order to get this information, the Co thin film on Si was prepared by IBAD method. The thickness of the prepared Co layer determined with TEM in KRISS was 1000 Å. Since one mass spectrum was taken for 500 laser shots at

Table 2. Impurity elements in commercial Zn sample

Impurity element	Concentration (ppm)
Cadmium (Cd)	1
Indium (In)	1
Copper (Cu)	less than 1
Iron (Fe)	less than 1
Silicon (Si)	less than 1
Silver (Ag)	less than 1

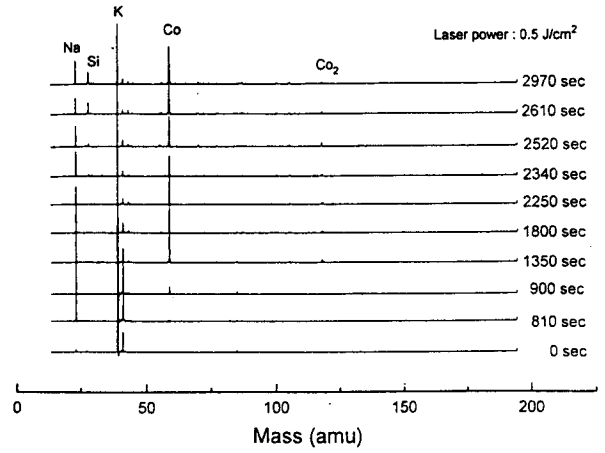

Figure 6. Part of the mass spectrum series of Co thin films on Si with the time interval of 90 sec obtained with the linear LIMS. Each spectrum has been taken for 50 sec from the starting time (shown in the right side of each spectrum). The experimental laser fluence and the peak assignments are also shown in the figure.

the repetition rate of 10 Hz, the information obtained from a mass spectrum is an average for 50 sec. While maintaining the averaging time per spectrum (50 sec) and the laser fluence (0.5 J/cm^2), a series of spectra were recorded at every 90 sec. Figure 6 presents the part of the mass spectrum series of the samples. The starting time of each spectrum is written on the right side of the spectrum so that each spectrum represents the averaged data for 50 sec after each starting time. In the first measurement starting at 0 sec (the bottom spectrum), only a trace amount of Co was observed with the impurities of Na and K. With increasing time, the intensity of Co peak became larger. The intensity of Co reached the maximum at the starting time of 1350 sec and stayed at almost the same value afterwards. This behavior is due to the conical shape of laser ablation. When the focused laser beam hits the surface of the sample for the first time, the effective area for the laser ablation corresponds to only the focal size of the beam spot. When the beam penetrates deeper, however, the effective area becomes larger till it reaches the maximum because the power of the laser beam edge is still high enough for the ablation, which is called the edge effect. This is why Co element kept being detected after Si element showed up in the mass spectrum. Si element did not show up until 2340 sec. These results imply that for the given laser power of 0.5 J/cm^2, it takes 2340 sec to dig out the Co layer. Assuming that the sputtering rate of laser ablation was constant all the way through the Co layer, about 20 Å thickness of the Co layer has been taken off for one mass spectrum. This means that

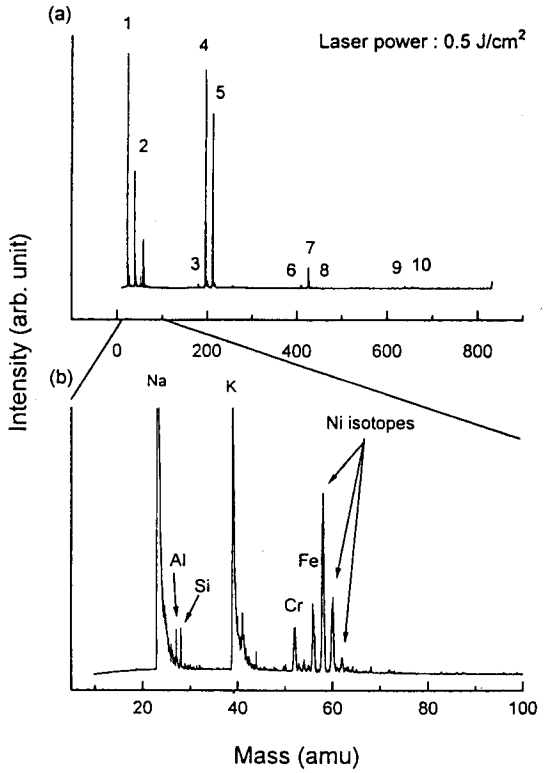

Figure 7. Mass spectrum of Ta_2O_5 thin films on Si (a) and the expanded spectrum (b) in the lower mass region. For details, see text.

each mass spectrum represents the information for the thickness of ~20 Å of the Co thin film.

For the identification of impurities in solid samples, two kinds of sample, Ta_2O_5 thin film on Si and PZT materials, were analyzed by the linear LIMS. In Figure 7(a), the mass spectrum of the Ta_2O_5 thin film is presented. In the spectrum, several peaks belonging to tantalum oxides are observed besides those of the surface contaminants of Na, K. The fragmented oxides and the larger clusters of Ta_2O_5 have been detected. The detailed assignments of the peaks are listed in Table 3. The expanded spectrum in the lower mass region is also shown in Figure 7(b). In this spectrum, some peaks not related to Ta_2O_5 appear. These peaks have been assigned to Al, Si, Cr, Fe, and Ni according to the mass and the isotope peaks pattern (marked in the figure). We found that the sample was contaminated by these elements from the target material. For PZT materials, two types of samples-thin film and bulk disk-were used. The mass spectra of PZT thin film and PZT bulk disk are shown in Figure 8(a) and Figure 8(b), respectively. In the spectra, the compositional elements of PZT, such as Pb, Zr, Ti and their oxides, are observed. The assignments of these major peaks are listed in Table 4. Since the isotope mass peaks are well-resolved for Ti, TiO, ZrO, and Pb, the main isotope peaks of them are assigned, such as ^{48}Ti, ^{48}TiO, etc. The intensities of Zr mass peaks are too low to resolve with the isotopes of Zr. Only a broad peak is observed at the mass position of Zr, even though ZrO has been detected clearly. For Pb, only the metal peak is observed while the PbO ion peak is too weak to be observed. In bulk PZT sample, the intensity of Pb ion is relatively strong, so the isotopes were not resolved by this spectrometer. Besides these peaks, several other peaks assigned in the Figure 8(b) have been detected. In the spectra of both thin film and bulk disk, we assign the strong peaks besides Zr compounds to Sr and its mono-oxide on the ground of the mass and the isotope peaks pattern. For Sr, the intensity of the metal peak is much stronger than that of its oxide. In the spectrum of bulk disk sample, the peak for mass 55 is determined to be for Mn. When the ratio of the peak intensities for TiO isotopes in Figure 8(a) is compared with that in Figure 8(b), one can easily realize that the peaks for mass 63 and 65 in Figure 8(b) are much stronger than those in Figure 8(a). And also the peaks for mass 126, 128, 130 are observed in

Table 3. List of the peak assignments of Ta_2O_5 thin films on Si

Peak #	Mass (amu)	Assignment
1	23	Na
2	39	K
3	181	Ta
4	197	TaO
5	213	TaO_2
6	410	Ta_2O_3
7	426	Ta_2O_4
8	442	Ta_2O_5
9	639	Ta_3O_6
10	655	Ta_3O_7

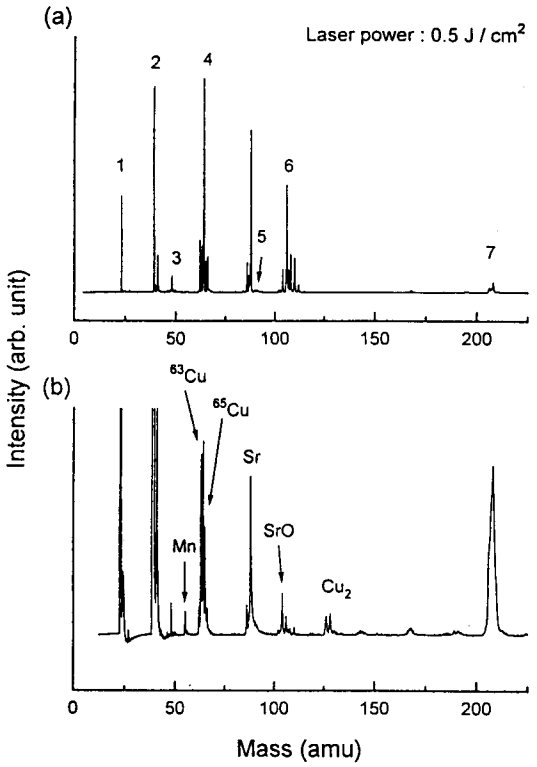

Figure 8. Mass spectrum of PZT thin film on platinized Si (a) and PZT bulk disk (b) taken by the linear LIMS. The peaks related to minor elements observed in PZT bulk disks are marked in the spectrum (b). The assignments of major elements are listed in Table 4.

Table 4. The list of the peak assignments of PZT samples

Peak #	Mass (amu)	Assignment
1	23	Na
2	39	K
3	48	^{48}Ti
4	64	^{48}TiO
5	91	Zr
6	106	^{90}ZrO
7	208	^{208}Pb

Figure 8(b). These peaks are typical peaks for Cu_2. From these observations, the peaks for mass 63 and 65 should be assigned to Cu isotopes. Since the masses of Cu isotopes are almost same as two isotopes of TiO compound, the peaks for Cu isotopes overlap with those for TiO. This is why the ratio of TiO isotopes measured in Figure 8(b) is quite different from the natural abundances. These impurities must be additives for PZT synthesis. Even though the PZT thin films were prepared from the PZT bulk disks by a pulsed laser deposition, Mn and Cu are not deposited to the thin film.

Summary and Conclusion

We have built and tested a laser ionization mass spectrometer (LIMS) which employs an Nd:YAG laser and a TOFMS. The method takes on the utmost capability when it is used for chemical composition analysis for solid samples. With this spectrometer, we have shown that the mass of higher than 2000 amu can be identified clearly and the mass resolution of 230 is achieved in the linear LIMS, which can be improved by employing a reflectron up to about 7 times in the present work. We have also reported the detection limit and the depth resolution of this spectrometry. The former is on the order of ppm for Fe and In. This represents the sensitivity of identifying impurities in the sample. Once the detection limits are determined for more elements, comparison with other analysis methods may well be made. The latter is about 20 Å/spectrum for Co film under our experimental conditions mentioned in the text. This number is also useful for quantitative analysis such as analysis of layer-by-layer multi-component films. Of course, to exercise the full capabilities of LIMS, more data for more standard samples should be obtained and accumulated. Therefore, we anticipate the application of LIMS be expanded into e.g. the analyses for binary alloys and polymers.

Acknowledgment. This work was supported by Ministry of Science and Technology. And also it was partly supported by the grants of (95-0501-09) from Korea Science and Engineering Foundation and (BSRI-96-6401) from Ministry of Education. We appreciate greatly Mr. K. J. Kim in KRISS for preparing Co and Ta_2O_5 thin films.

Reference

1. (a) Czanderna, A. W. In *Methods of Surface Characterization. Volume 2, Ion Spectroscopies For Surface Analysis*; Czanderna, A. W.; Hercules, D. M., Ed.; Plenum Press: New York, U. S. A., 1991, p 37. (b) Denoyer, E.; Van Grieken, R.; Adams, F.; Natusch, D. F. S. *Anal. Chem.* **1982**, *54*, 26A.
2. Odom, W. R.; Schueler, B. In *Laser and Mass Spectrometry*; Lubman, D. M., Ed.; Oxford University Press, Oxford, 1990, p 105.
3. Wilky, Z. A.; Hercules, D. M. *Anal. Chem.* **1987**, *59*, 1819.
4. Consalvo, D.; Mele, A.; Stranges, D.; Giardini-Guidoni, A.; Teghil, R. *Int. J. Mass Spectrom. Ion Process* **1989**, *91*, 319.
5. (a) Seydel, U.; Lindner, B. In *Microbeam Analysis-1987*; Geiss, R. H., Ed.; San Francisco Press, San Francisco, 1987, p 353. (b) Cotter, R. J. *Anal. Chem.* **1992**, *64*, 1027A.
6. (a) Cotter, R. J. *Anal. Chimica Acta* **1987**, *85*, 195. (b) Gentry, W. R.; Giese, C. F. *Rev. Sci. Instrum.* **1978**, *49*, 595.
7. Cotter, R. J. In *ACS SYPOSIUM Series 549. Time-of-Flight Mass Spectrometry*; Cotter, R. J. Ed.; American Chemical Society, Washington, D. C., 1994; p 17.
8. Mamyrin, B. A.; Karataev, V. I.; Shmikk, D. V.; Zagulin, V. A. *Sov. Phys. JETP* **1973**, *45*, 37.
9. Manuscript in preparation. Im, H.-S.; Shin, D. N.; Chung, K. H. Design parameters for a reflectron in Time-of-Flight Mass Spectrometer.
10. Bosel, U.; Weinkauf, R.; Schlag, E. W. *Int. J. Mass Spectrum, Ion Process* **1992**, *112*, 121.
11. Vredun, F. R.; Krier, G.; Alurber, J. F. *Anal. Chem.* **1987**, *59*, 1383.
12. Im, H.-S.; Yoon, H.-S.; Kim, S. K. unpulished results.